Physics Letters B 738 (2014) 519–523

Contents lists available at ScienceDirect

Physics Letters B

www.elsevier.com/locate/physletb

Pygmy dipole resonance in ^{124}Sn populated by inelastic scattering of ^{17}O

L. Pellegri [a,b], A. Bracco [a,b,*], F.C.L. Crespi [a,b], S. Leoni [a,b], F. Camera [a,b], E.G. Lanza [c], M. Kmiecik [d], A. Maj [d], R. Avigo [a,b], G. Benzoni [a], N. Blasi [a], C. Boiano [a], S. Bottoni [a,b], S. Brambilla [a], S. Ceruti [a,b], A. Giaz [a], B. Million [a], A.I. Morales [a,b], R. Nicolini [a,b], V. Vandone [a,b], O. Wieland [a], D. Bazzacco [e], P. Bednarczyk [d], M. Bellato [e], B. Birkenbach [f], D. Bortolato [e,g], B. Cederwall [h], L. Charles [i], M. Ciemala [d], G. De Angelis [j], P. Désesquelles [k], J. Eberth [f], E. Farnea [e], A. Gadea [l], R. Gernhäuser [m], A. Görgen [n], A. Gottardo [g,j], J. Grebosz [d], H. Hess [f], R. Isocrate [e], J. Jolie [f], D. Judson [o], A. Jungclaus [p], N. Karkour [k], M. Krzysiek [d], E. Litvinova [q,r], S. Lunardi [e,g], K. Mazurek [d], D. Mengoni [e,g], C. Michelagnoli [e,g,1], R. Menegazzo [e,g], P. Molini [e,g], D.R. Napoli [j], A. Pullia [a,b], B. Quintana [s], F. Recchia [e,g], P. Reiter [f], M.D. Salsac [t], B. Siebeck [f], S. Siem [n], J. Simpson [u], P.-A. Söderström [v,2], O. Stezowski [w,x,y], Ch. Theisen [t], C. Ur [e], J.J. Valiente Dobon [j], M. Zieblinski [d]

[a] INFN Sezione di Milano, I-20133 Milano, Italy
[b] Dipartimento di Fisica, Università degli studi di Milano, I-20133 Milano, Italy
[c] INFN Sezione di Catania, I-95123 Catania, Italy
[d] The Henryk Niewodniczański Institute of Nuclear Physics, PAN, 31-342 Krakow, Poland
[e] INFN Sezione di Padova, I-35131 Padova, Italy
[f] Institut für Kernphysik, Universität zu Köln, D-50937 Köln, Germany
[g] Dipartimento di Fisica e Astronomia, Università degli studi di Padova, I-35131 Padova, Italy
[h] Department of Physics, Royal Institute of Technology, SE-10691 Stockholm, Sweden
[i] Institut Pluridisciplinaire Hubert Curien – IPHC, CNRS/IN2P3 and Université de Strasbourg, BP 28, F-67037 Strasbourg Cedex 2, France
[j] INFN, Laboratori Nazionali di Legnaro, I-35020 Padova, Italy
[k] Centre de Spectrométrie Nucléaire et de Spectrométrie de Masse – CSNSM, CNRS/IN2P3 and Univ. Paris-Sud, F-91405 Orsay Campus, France
[l] IFIC, CSIC, Universitat de València, E-46980 València, Spain
[m] Physics Department E12, Technische Universität München, James-Franck-Straße. 1, D-85748 Garching, Germany
[n] Department of Physics, University of Oslo, N-0316 Oslo, Norway
[o] Oliver Lodge Laboratory, The University of Liverpool, Liverpool, L69 7ZE, UK
[p] Instituto de Estructura de la Materia, CSIC, E-28006 Madrid, Spain
[q] Department of Physics, Western Michigan University, Kalamazoo, MI 49008-5252, USA
[r] National Superconducting Cyclotron Laboratory, Michigan State University, East Lansing, MI 48824-1321, USA
[s] Laboratorio de Radiaciones Ionizantes, Universidad de Salamanca, E-37008 Salamanca, Spain
[t] Institut de Recherche sur les lois Fondamentales de l'Univers – IRFU, CEA/DSM, Centre CEA de Saclay, F-91191 Gif-sur-Yvette Cedex, France
[u] STFC Daresbury Laboratory, Daresbury, Warrington, WA4 4AD, UK
[v] Department of Physics and Astronomy, Uppsala University, SE-75120 Uppsala, Sweden
[w] Université de Lyon, F-69622 Lyon, France
[x] Université Lyon 1, Villeurbanne, France
[y] CNRS/IN2P3, UMR5822, IPNL, France

ARTICLE INFO

Article history:
Received 8 July 2014
Received in revised form 6 August 2014
Accepted 12 August 2014
Available online 15 August 2014
Editor: V. Metag

ABSTRACT

The γ decay from the high-lying states of ^{124}Sn was measured using the inelastic scattering of ^{17}O at 340 MeV. The emitted γ rays were detected with high resolution with the AGATA demonstrator array and the scattered ions were detected in two segmented ΔE–E silicon telescopes. The angular distribution was measured both for the γ rays and the scattered ^{17}O ions. An accumulation of E1 strength below the particle threshold was found and compared with previous data obtained with (γ,γ') and $(\alpha,\alpha'\gamma)$ reactions. The present results of elastic scattering, and excitation of E2 and E1 states were analysed

* Corresponding author at: Dipartimento di Fisica, Università degli studi di Milano, I-20133 Milano, Italy. Tel.: +39 02 50317252.
E-mail address: angela.bracco@mi.infn.it (A. Bracco).

http://dx.doi.org/10.1016/j.physletb.2014.08.029

Keywords:
Low-lying electric dipole excitations
^{124}Sn
Isospin character

using the DWBA approach. From this comprehensive description the isoscalar component of the 1^- excited states was extracted. The obtained values are based on the comparison of the data with DWBA calculations including a form factor deduced using a microscopic transition density.

In atomic nuclei, the isovector electric dipole strength is almost completely exhausted by the isovector giant dipole resonance (IVGDR), located in the energy range between 10–20 MeV. However, in particular in the case of neutron-rich nuclei, a few percent of this strength is found in the so-called Pygmy Dipole Resonance (PDR), a concentration of 1^- states located around the particle threshold [1]. The study of the PDR is not only interesting as a phenomenon associated to the nuclear structure, but it also has astrophysical implications. Indeed, pygmy states are expected to provide information on the neutron skin and, as a consequence, on the symmetry energy term of the equation of state [2–6]. Furthermore, the occurrence of low-lying dipole strength plays an important role in predictions of neutron-capture rates in the r-process nucleosynthesis, and consequently in the calculated element abundance distribution. Due to the fact that the PDR is located close to the neutron threshold, it can significantly enhance the radiative neutron-capture cross section on neutron-rich nuclei [7].

A simple interpretation of the electric dipole excitation is given by the three-fluid hydrodynamical model [8]. Within this model, two independent electric dipole resonances are naturally found, one originating from the oscillation of all protons against all neutrons (GDR) and the other described as an excess of neutrons which oscillate against a $N = Z$ core (PDR). Several microscopic models, reported in a recent review [9], were then developed to describe, in detail, the properties of this excitation mode. The transition densities for these dipole states were found to all have a common feature, namely that neutrons and protons are in phase inside the nucleus while at the surface only some neutrons contribute. Consequently, these states seem to be characterised by a strong mixing of isospin components. In this respect it is important to underline the results of recent works comparing data from photon and α-scattering experiments which show a different behaviour in the population of these states [10–12]. Indeed, a set of states in the low energy part of the pygmy region is excited with both types of reactions, while the states at higher energies are not populated by α-scattering. This splitting in the population of the states reveals a different underlying structure: the low energy part seems to have a more isoscalar character dominated by neutron-skin oscillations, while the high-energy states are mainly of isovector nature associated to a transition towards the GDR.

In spite of the experimental and theoretical efforts, the nature of low-lying E1 excited states is still under debate and thus, to progress in this direction, new experimental data using different probes are needed. This paper aims at a detailed study of the PDR in ^{124}Sn using the (^{17}O,^{17}O$'\gamma$) reaction having, in particular, two main goals: the first is to check with a different probe the observed splitting of the PDR and the second is to obtain the fraction of the isoscalar energy weighted sum rule (ISEWSR) exhausted by the pygmy states in this nucleus, by performing a DWBA analysis of the data. With the use of ^{17}O at bombarding energy where the nuclear isoscalar excitation is dominant and the comparison with data from γ and α probes is possible, one expects to get better insight into the mixing of isoscalar and isovector components. Indeed, an accurate choice of projectile mass, charge, bombarding energy and scattering angle, allows one to modify the relative role of the nuclear and Coulomb components needed to test the mixed nature displayed by these states [13]. The use of ^{17}O has been recently demonstrated to be a good choice by a work investigating the pygmy states in ^{208}Pb. In this work the isoscalar strength in several E1 states of ^{208}Pb was obtained [14]. In addition there is strong interest in the study of the dependence of the E1 strength with increasing neutron number and the Sn isotopic chain offers this opportunity [15,16]. Therefore the present work on ^{124}Sn is interesting in this connection.

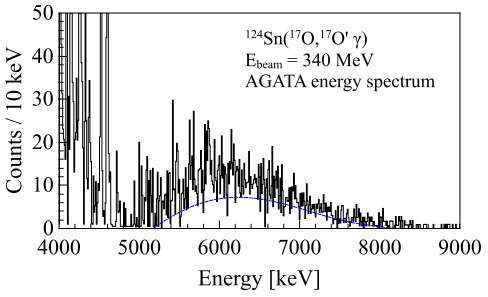

Fig. 1. γ-Ray energy spectrum of ^{124}Sn in the PDR region measured with AGATA and obtained with the gating conditions on the excitation energy measured with the inelastic scattered particles, as described in the text.

The experiment was performed at the Tandem-ALPI accelerator complex of the Legnaro National Laboratories (LNL-INFN) in Italy. A beam of ^{17}O ions at 340 MeV in the laboratory frame, impinged on a self-supporting ^{124}Sn target with a thickness of 3 mg/cm^2. A crucial point in the studies of the pygmy dipole resonance via inelastic scattering of heavy ions is the proper choice of the projectile. Indeed, both target and projectile excitations can occur and one has to be able to separate them. The ^{17}O nucleus is a very suitable projectile for this type of experiments because it is loosely bound (the neutron separation energy being 4.1 MeV). Consequently, the detection of the ^{17}O in the outgoing channel, ensures that the γ rays in the energy region of interest, 5–9 MeV, are mainly associated to the de-excitation of the target and not of the projectile. The detection of the scattered ions was performed with two segmented ΔE–E Silicon telescopes (pixel type), prototypes of the TRACE project [17,18]. They were placed symmetrically with respect to the beam axis. The angular range covered by these telescopes was of 9°–22°, and they allowed for a good separation of the ions. The total energy resolution for the summed signals was ∼0.4% at this beam energy. The γ rays produced from the de-excitation of the reaction participants were measured with high resolution with the highly-segmented HPGe detectors of the AGATA Demonstrator system [18–20]. This array consisted of 5 triple clusters grouped together and placed at a distance of 132 mm. Its axis, passing from the geometrical centre, formed an angle of 72° with respect to the beam direction.

The γ-ray energy spectrum measured with the AGATA demonstrator array in the region of the pygmy resonance is shown in Fig. 1. This spectrum was obtained after applying gating conditions to select inelastically scattered ^{17}O events and decays to ground state. For this purpose, a correlation between the γ-ray

[1] Current address: GANIL, CEA/DSM-CNRS/IN2P3, Boulevard H. Becquerel, F-14076, Caen, France.

[2] Current address: RIKEN Nishina Center, 2-1 Hirosawa, Wako, 351-0198 Saitama, Japan.

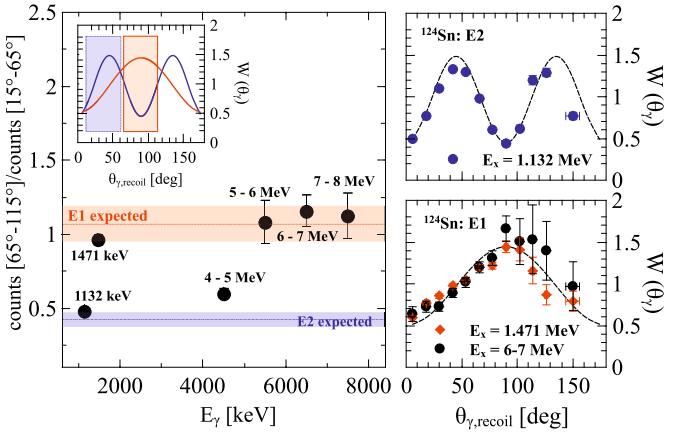

Fig. 2. Left panel: Ratio between the number of counts in the 65°–115° angular range (red region in the inset) over the number of counts in the 15°–65° angular range (blue region in the inset), measured with the AGATA Demonstrator, for different transitions of ^{124}Sn. The horizontal red and blue bands correspond to the expected ratio for E1 and E2 transitions, respectively. The widths of the horizontal bands reflect the uncertainty in the spin alignment deduced from the angular distribution fit of the 1.132 MeV and the 1.471 MeV data. Right panels: Angular distributions for different E2 (top) and E1 (bottom) γ-ray transitions. (For interpretation of the references to color in this figure, the reader is referred to the web version of this article.)

energy and the excitation energy transferred to the target was imposed. The target excitation energy was obtained as the total kinetic energy loss of the scattered ^{17}O ions. To this end, by applying a diagonal gate ($E_x = E_\gamma$) on the matrix of the measured decay energy versus the excitation energy, it was possible to select in the γ-ray energy spectrum only the transitions to the ground state. To reject accidental background and feeding from higher-lying states we constructed a spectrum with another diagonal gate centred at $E_x = E_\gamma + 2$ MeV and with the same width of 2 MeV. The obtained spectrum (that was subtracted from the one corresponding to the $E_x = E_\gamma$ condition) shows negligible counts in the region above 5 MeV. Indeed, this is expected because it is known that this resonance is characterised by a number of discrete 1^- states whose dominant decay is towards the ground state. Finally, since the typical lifetime of these states is of the order of femtoseconds, a Doppler correction for the recoil motion was also applied. The energy spectrum of Fig. 1 is characterised by a large fragmentation of the dipole strength similar to what was previously observed in the α-scattering experiment [11]. In this spectrum several E1 transitions known from (γ,γ') and $(\alpha,\alpha'\gamma)$ measurements [10, 11] were identified.

Exploiting the position sensitivity of the AGATA Demonstrator array and of the segmented silicon telescopes it was possible to obtain an almost continuous angular distribution for the emitted γ rays. The information on the interaction point of the ^{17}O ion in the silicon telescopes and that of the γ ray measured with the AGATA Demonstrator was used to reconstruct the angle between the ^{124}Sn recoil and the associated γ-ray emission. Fig. 2 shows the angular distributions obtained for different E1 and E2 transitions. On the right hand side, the top panel shows the angular distribution for the E2 transition at 1.132 MeV (blue dots). The bottom panel shows two angular distributions one corresponding to the E1 transition at 1.471 MeV (red diamonds) and the other to the integrated region between 6–7 MeV (black dots) where PDR transitions are located. From Fig. 2 one sees that the angular distributions follow the expected trend for each multipolarity. It must be underlined that due to the low statistics of the recoils detected in the left silicon telescopes, the angular distributions between 90°–180° are dominated by statistical fluctuations.

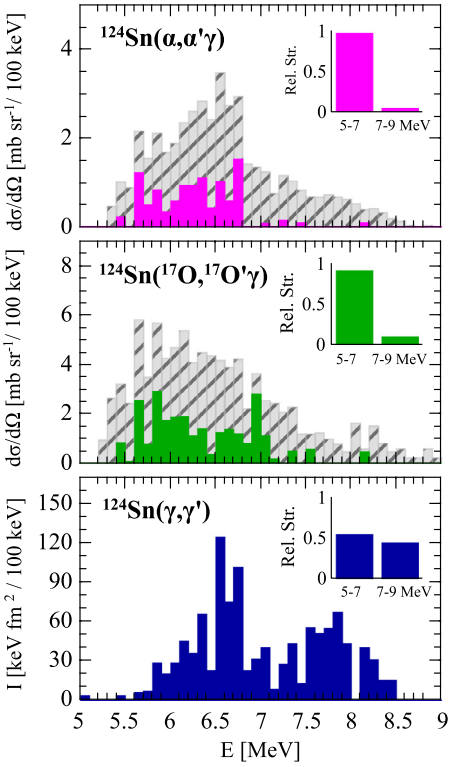

Fig. 3. Differential cross sections measured in the ^{124}Sn(^{17}O,^{17}O$'\gamma$) experiment, in bins of 100 keV (central panel). The unresolved strength, corresponding to the total binned counts in the measured spectra, is depicted in grey. For comparison, the strengths measured in α-scattering (top panel) [12] and photon-scattering (bottom panel) [10] are reported. In each panel, the inset gives the relative intensity corresponding to the measured cross sections in the discrete lines integrated in two regions 5–7 and 7–9 MeV.

The ratio between the number of counts in the red (65°–115°) and in the blue (15°–65°) regions as illustrated in the inset of the left panel of Fig. 2 was computed for transitions in different energy regions to deduce their multipolarities. The left panel of Fig. 2 clearly shows that the region of the PDR (between 5.5 and 8 MeV) has the characteristic E1 behaviour, in agreement with previous observations based on other probes [12]. Concerning the possible M1 contribution, we used the information from the (γ,γ') work [10] giving tentative assignments for two transitions at 6.808 and 8.269 MeV and concluding that the M1 contribution amounts to less then 10% of the total dipole strength. In particular, in the present case we don't identify these two transitions supposedly due to the combined effect of their weak intensity and of the high density of states in the region of interest.

One of the crucial points of this work is the comparison of the presently measured cross sections with (γ,γ') and $(\alpha,\alpha'\gamma)$ results. This comparison is presented in Fig. 3 showing the differential cross sections associated to the ground-state decay spectrum with data in bins 100 keV wide. In the case of (^{17}O,^{17}O$'\gamma$) and $(\alpha,\alpha'\gamma)$ data, for each 100 keV bin two cross sections are shown: one corresponding to the counts in the known discrete peaks (full coloured bars) and the other to the total measured counts denoted as unresolved strength (dashed grey bars). From this figure one sees clearly, also in the present data, the splitting of the PDR states in two regions as in the $(\alpha,\alpha'\gamma)$ data (top panel). This is due to the different nature of these states: the low-lying part of the E1 strength appears to be characterised by isoscalar transition densities that are peaked on the surface which lead to an enhancement in the isoscalar E1 response, while the higher-lying states can be interpreted as transitions towards the GDR and, thus, are

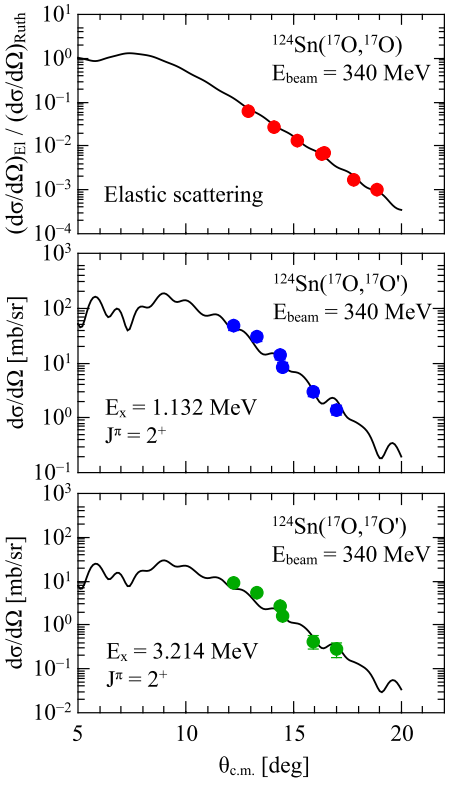

Fig. 4. Experimental cross sections (filled circles) and DWBA calculations (solid curves) for the elastic and inelastic scattering of ^{17}O on ^{124}Sn at $E_{beam} = 340$ MeV. Top panel: elastic scattering differential cross section divided by the Rutherford cross section. Cross sections are shown for the 2$^+$ excited states at 1.132 MeV (central panel) and 3.214 MeV (bottom panel). The statistical error is given by the error bars.

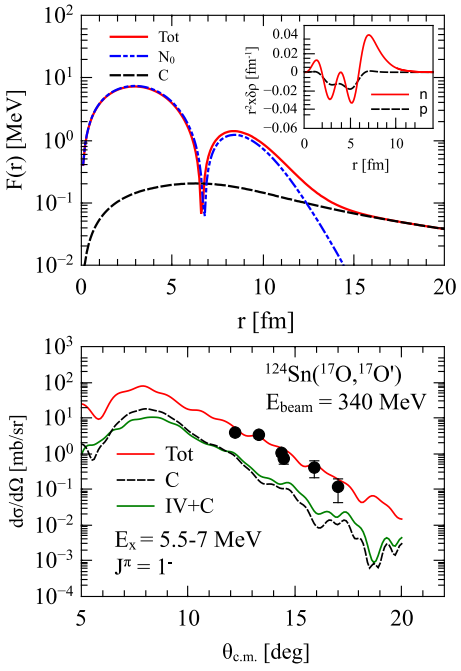

Fig. 5. Top panel: Form factor associated to the PDR states for the ^{124}Sn+^{17}O system. The Coulomb (black dashed line) and the nuclear (blue dashed line) components are shown together with the total one (red solid line). Bottom panel: differential cross sections for the 1$^-$ states between 5.5–7 MeV. The black dashed line shows the DWBA calculation with the Coulomb contribution only; the green solid line is a DWBA calculation including both the Coulomb and nuclear contributions with a form factor of GDR type; the red solid line (reproducing well the data) uses the total form factor shown in the top panel of the figure. (For interpretation of the references to color in this figure, the reader is referred to the web version of this article.)

suppressed in the isoscalar channel [12]. The splitting of the PDR region becomes even more evident if we integrate the strength in the discrete peaks measured in each experiment into two regions, 5–7 and 7–9 MeV (insets of Fig. 3). From here one sees clearly that the strengths in the two regions measured in the (γ,γ') experiment are almost equal while this is not the case for the $(^{17}\mathrm{O},^{17}\mathrm{O}'\gamma)$ and $(\alpha,\alpha'\gamma)$ experiments. The small relative difference between $(\alpha,\alpha'\gamma)$ and $(^{17}\mathrm{O},^{17}\mathrm{O}'\gamma)$ in the population cross section of some states might be related to the nature of these states and to the different Coulomb and nuclear contributions in these reactions.

In order to extract quantitatively the isoscalar strength of these pygmy states a distorted wave Born approximation (DWBA) analysis was performed for the present measurements of the differential cross sections at different scattering angles. The DWBA calculations were performed using the computer code FRESCO [21]. Since a not well calibrated Faraday cup was available, the combined contribution of the beam current and target thickness was deduced by normalising the data to the elastic scattering cross section calculations. This normalization factor was used for every inelastic scattering cross sections measured at the same time. Fig. 4 (top panel) shows the data obtained for the elastic scattering divided by the Rutherford cross section. The optical model parameters of the Woods–Saxon potentials that best fitted our data were, for the depth of the real and imaginary potentials, $V = 50.0$ MeV and $W = 32.0$ MeV and for the radii and the diffusenesses of the real and imaginary parts $r_v = r_w = 1.16$ fm and $a_v = a_w = 0.67$ fm, respectively. The Coulomb radius parameter was $r_c = 1.2$ fm. To check the reliability and the accuracy of our calculations, a comparison between the experimental and the calculated cross sections for different 2$^+$ excited states was made. The calculations for the excited states used the standard collective-model form factor, namely a deformed Woods–Saxon potential employed in the FRESCO code. For the excited states calculations the known $B(\mathrm{E}\lambda)\uparrow$ values [10,22] were used. The central and bottom panels of Fig. 4 show the experimental differential cross sections for the excitation of the collective 2$^+$ states of ^{124}Sn at 1.132 MeV and 3.214 MeV, respectively, in comparison with the calculations. These predictions were obtained assuming pure isoscalar excitation implying that the ratio of the neutron matrix element M_n and proton matrix element M_p is given by $M_n/M_p = N/Z$. It is clear from this figure that the calculated curves are in excellent agreement with the data, and support the interpretation of a pure isoscalar nature of these states.

The DWBA analysis of the E1 states is presented in the bottom panel of Fig. 5. Since the statistics was insufficient to get an angular distribution of the scattered particles for each separate state, the data were integrated in the excitation energy region 5.5–7 MeV. The cross-section calculations for the Coulomb excitation (very similar to the total excitation using for the nuclear part the standard collective model form factor [21]) in the region between 5.5–7 MeV are shown with the black dashed line, in comparison with the data (bottom panel of Fig. 5). The used value for the summed B(E1) was 0.22 W.u. A calculation including both the Coulomb and nuclear contributions and corresponding to a form factor of GDR type is shown with the green solid line in the bottom panel of Fig. 5. A large disagreement between data and these two calculations is found. In particular, the cross section associated to a pure Coulomb excitation only accounts for less then 10% of the measured yield. This leads us to conclude that the main contribution to the inelastic excitation at our beam energy comes from the

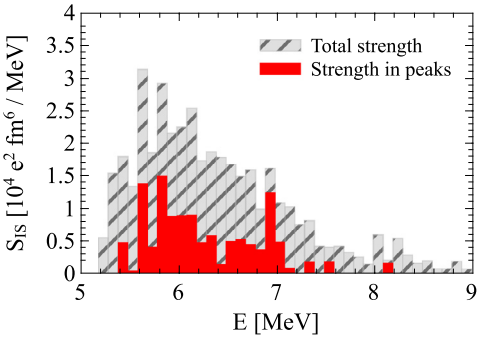

Fig. 6. Isoscalar strength distribution obtained for the PDR states, integrated in bins of 100 keV. The full coloured bars correspond to the sum of known discrete transitions in each energy bin. The dashed grey bars give the total strength (including the unresolved part) corresponding to the total counts in each energy bin. In both cases the predicted Coulomb contribution was subtracted.

nuclear part which needs a nuclear form factor for these states different than that of GDR type. Consequently, another DWBA calculation was performed (red solid line) using a microscopic form factor based on the transition density associated to the E1 pygmy states obtained with a relativistic quasiparticle time-blocking approximation (RQTBA) microscopic model [23]. The latter is based on covariant energy-density functional theory with single-particle and vibrational degrees of freedom coupling yielding an extension beyond the mean-field approach. Such transition density is shown in the inset of the top panel of Fig. 5 for protons and neutrons. It is evident from its shape that the external region is dominated by the neutron contribution. For the calculation of the form factor a double folding procedure with an M3Y nucleon–nucleon interaction was used [24]. This form factor as well as the used transition densities (in the inset) are shown in the top panel of Fig. 5. As expected for these states, the dominant contribution to the form factor comes from the isocalar part of the nucleon–nucleon interaction component. The calculations based on the microscopic form factor were fitted to the data to extract the value of the ISEWSR strength. In particular, it has been assumed that the cross section is a sum of two parts, one being the Coulomb and the other the nuclear (isoscalar) contribution. For the Coulomb contribution we fixed the value corresponding to the known B(E1) measurements [10]. For the nuclear contribution fitting the data the starting value was that associated to the used microscopic form factor corresponding to 0.5% of the ISEWSR strength (2.17×10^3 $e^2\,\mathrm{fm}^6$). Indeed 0.5% of the ISEWSR is the ratio of the values obtained by applying the isoscalar dipole operator [12] to a state at 7.1 MeV (the most intense in the region of interest) and to all calculated states up to 50 MeV. Since the value of the fraction of the ISEWSR is proportional to the isoscalar cross section, we multiplied this value to fit the experimental cross section data and this resulted in 1.5 (0.2)% of the ISEWSR strength for the sum of the measured discrete states in the interval 5.5–7 MeV.

Fig. 6 reports (using red bars) the energy distribution of the isoscalar strength values in $e^2\,\mathrm{fm}^6$/MeV based on the results of the data fitting shown in Fig. 5. The data are integrated in bins of 100 keV. It is clear that a sizable isoscalar dipole strength characterises the low energy part (below 7 MeV) of the 1^- states. This picture is confirmed also by the measured distribution corresponding to the total unresolved strength, displayed with grey bars in Fig. 6. These experimental results are in general agreement with the corresponding predictions based on the RQTBA microscopic model [12,24], although the calculated states are shifted up in excitation energy by about 2 MeV as compared with the data. In addition, the present data are consistent with the results of experiments focusing on the ISGDR at around 20 MeV, where most of the isoscalar strength is located [25,26]. In fact, the total measured strength in the discrete peaks is 2.2 (0.3)% of the EWSR and 7.8 (0.7)% for the unresolved region.

In summary, we have presented the results of an experiment aimed at the investigation of the isospin character of dipole states in ^{124}Sn in the region below the neutron binding energy. The ^{17}O probe at around 20 MeV/u resulted to be a good tool for this purpose. The data are in remarkable agreement with a previous experiment using the $(\alpha, \alpha'\gamma)$ inelastic scattering reaction. Both reactions are selective in the population of specific pygmy states as compared to photon-scattering. In addition, this experiment provided the isoscalar strength distribution of the pygmy states. Indeed, the angular distribution measurements of the emitted γ rays and of the scattered ^{17}O ions corresponding to the ground and different excited states are found to be essential in this connection. For the 1^- states a DWBA analysis based on a microscopically calculated form factor was performed and showed a sensitivity to the surface part of the transition density. Being the transition density dominated on the surface by the neutron component one can deduce that the pygmy states ^{124}Sn are associated with the excitation of surface neutrons, mainly those in the neutron skin. Therefore in the future it will be very interesting to perform these studies on the isotopic chain of Sn and other neutron-rich nuclei also using other probes as protons at medium energy.

Acknowledgements

The following support is acknowledged: (i) the Italian Institute of Nuclear Physics; (ii) the Polish Ministry of Science and Higher Education under Grant No. 2011/03/B/ST2/01894; (iii) the National Superconducting Cyclotron Laboratory at MSU; (iv) the US NSF Grant PHY-1204486; and the German BMBF under Grant 06KY9136.

References

[1] D. Savran, et al., Prog. Part. Nucl. Phys. 70 (2013) 210.
[2] A. Klimkiewicz, et al., Phys. Rev. C 76 (2007) 051603.
[3] A. Carbone, et al., Phys. Rev. C 81 (2010) 041301(R).
[4] X. Roca-Maza, et al., Phys. Rev. Lett. 106 (25) (2011) 252501.
[5] A. Tamii, et al., Phys. Rev. Lett. 107 (2011) 062502.
[6] O. Wieland, et al., Phys. Rev. Lett. 102 (9) (2009) 092502.
[7] S. Goriely, et al., Nucl. Phys. A 739 (2004) 331.
[8] R. Mohan, et al., Phys. Rev. C 3 (1971) 1740.
[9] N. Paar, et al., Rep. Prog. Phys. 70 (2007) 691.
[10] K. Govaert, et al., Phys. Rev. C 57 (1998) 2229.
[11] J. Endres, et al., Phys. Rev. Lett. 105 (2010) 212503.
[12] J. Endres, et al., Phys. Rev. C 85 (2012) 064331.
[13] E.G. Lanza, et al., Phys. Rev. C 84 (2011) 064602.
[14] F.C.L. Crespi, et al., Phys. Rev. Lett. 113 (2014) 012501.
[15] N. Tsoneva, H. Lenske, Phys. Rev. C 77 (2008) 024321.
[16] P. Adrich, et al., Phys. Rev. Lett. 95 (2005) 132501.
[17] A. Gadea, et al., Nucl. Instrum. Methods Phys. Res., Sect. A, Accel. Spectrom. Detect. Assoc. Equip. 654 (2011) 88.
[18] S. Akkoyun, et al., Nucl. Instrum. Methods Phys. Res., Sect. A, Accel. Spectrom. Detect. Assoc. Equip. 668 (2012) 26.
[19] F.C.L. Crespi, et al., Nucl. Instrum. Methods Phys. Res., Sect. A, Accel. Spectrom. Detect. Assoc. Equip. 705 (2013) 47.
[20] E. Farnea, et al., Nucl. Instrum. Methods Phys. Res., Sect. A, Accel. Spectrom. Detect. Assoc. Equip. 621 (2010) 331.
[21] I.J. Thompson, et al., Comput. Phys. Rep. 7 (1988) 167.
[22] H. Iimura, et al., Nucl. Data Sheets 80 (1987) 111.
[23] E. Litvinova, et al., Phys. Rev. C 78 (2008) 014312.
[24] E.G. Lanza, et al., Phys. Rev. C 89 (2014) 041601(R).
[25] T. Li, et al., Phys. Rev. C 81 (2010) 034309.
[26] D.H. Youngblood, et al., Phys. Rev. C 69 (2004) 034315.